Research Square

Preprints are preliminary reports that have not undergone peer review.
They should not be considered conclusive, used to inform clinical practice,
or referenced by the media as validated information.

Nutrient Availability Shifts Biomass and Lipid Allocation in Scenedesmus obliquus: Dose Responses to Nitrogen, Phosphate and Iron

Abideen. A. Adekanmi

abideenadekanmi@gmail.com

University of Ibadan (IU)

Emmanuel. O. Garuba

University of Ibadan (IU)

Hidayat. A. Adekanmi

Federal Polytechnic Ede

Research Article

Keywords:

Posted Date: November 11th, 2026

DOI: https://doi.org/10.21203/rs.3.rs-11486606/v1

License: This work is licensed under a Creative Commons Attribution 4.0 International License.
Read Full License

Additional Declarations: No competing interests reported.

Nutrient Availability Shifts Biomass and Lipid Allocation in *Scenedesmus obliquus*: Dose Responses to Nitrogen, Phosphate and Iron

[*]Abideen. A. Adekanmi [1], Emmanuel. O. Garuba[1], Hidayat. A. Adekanmi[2]

[1] Department of Microbiology, University of Ibadan (IU), Ibadan, Oyo State, Nigeria

[2]Department of Nutrition and Dietetics, Federal Polytechnic Ede, Nigeria

[*]Correspondence: Department of Microbiology, University of Ibadan (IU), Ibadan, Oyo State, Nigeria

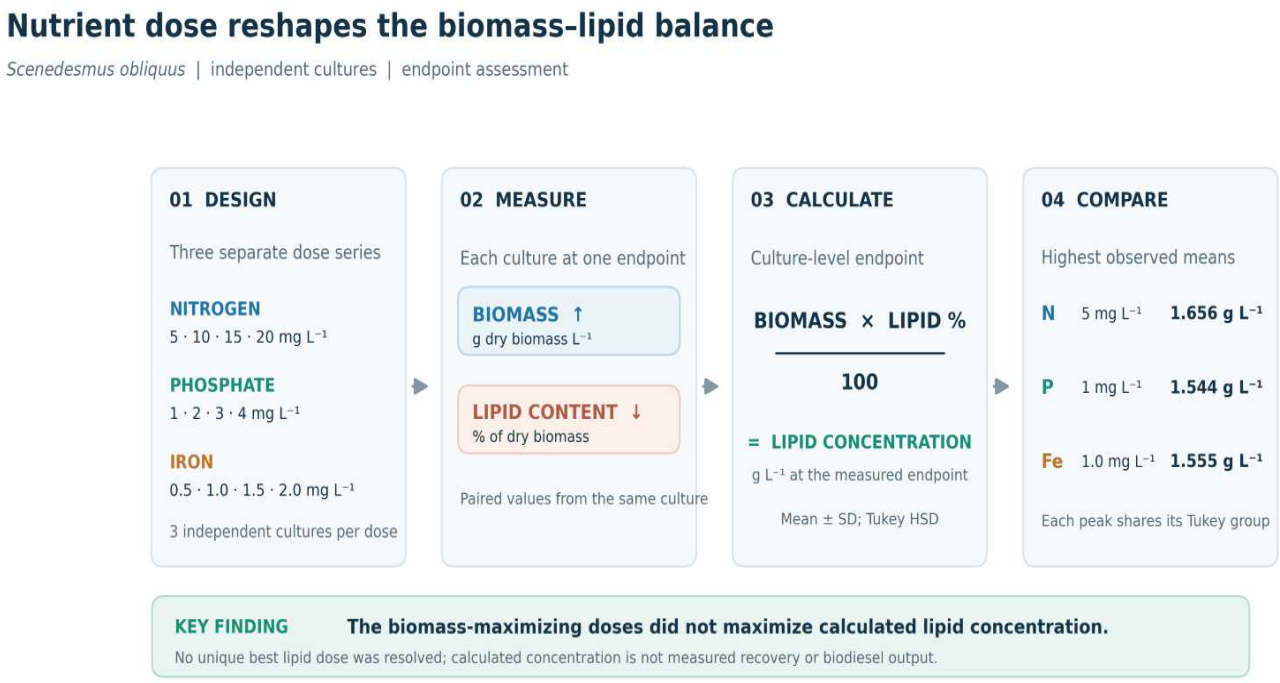
Email: yinklab1234gmail.com & abideenadekanmi@gmail.com

Highlights:

- Biomass rose by 33.8–35.7% across the three nutrient dose series.
- Lipid content fell by 22.63–25.45 percentage points across the series.
- Peak calculated lipid concentrations were 1.656, 1.544 and 1.555 g L^{-1}.

- The highest nutrient doses gave the greatest biomass, but fewer lipids per litre.
- Tukey tests did not identify a unique best dose for lipid concentration.

Graphical Abstract



Graphical Abstract

Nutrient-dose studies often identify a preferred microalgal cultivation condition from biomass concentration or lipid percentage alone. Because these responses can move in opposite directions, either measure may give an incomplete picture of lipid amount per culture volume. This study therefore aimed to compare biomass, lipid content and calculated endpoint lipid concentration across separate nitrogen, phosphate and iron dose series in *Scenedesmus obliquus*, and to determine whether the dose favoured depended on the endpoint assessed. Nitrogen (5–20

mg L^{-1}), phosphate (1–4 mg L^{-1}) and iron (0.5–2.0 mg L^{-1}) were each tested at four doses, with three independently cultivated cultures per dose. Biomass concentration and lipid content were measured; lipid concentration was calculated from their paired values for each culture. Within-series differences were assessed by one-way ANOVA and Tukey's test. Biomass increased with dose, reaching 2.877 ± 0.025, 2.777 ± 0.025 and 2.863 ± 0.015 g L^{-1} at the highest nitrogen, phosphate and iron doses, respectively. Lipid content declined from 77.03 ± 1.17 to 51.58 ± 0.73%, 74.83 ± 0.70 to 52.20 ± 0.36%, and 73.00 ± 0.20 to 50.13 ± 0.25% across the respective series. The highest observed calculated lipid concentrations were 1.656 ± 0.048 g L^{-1} at 5 mg L^{-1} nitrogen, 1.544 ± 0.026 g L^{-1} at 1 mg L^{-1} phosphate and 1.555 ± 0.017 g L^{-1} at 1.0 mg L^{-1} iron. None was statistically distinct from all neighbouring lower-dose treatments. The dose that maximized biomass did not maximize calculated lipid concentration in any series. The findings support endpoint-specific dose selection, while the pairwise comparisons do not establish a unique lipid-concentration optimum. Calculated endpoint concentration does not establish lipid productivity or recovered product output.

Keywords: *Scenedesmus obliquus*; nitrogen; phosphate; iron; biomass concentration; lipid content; calculated lipid concentration

1. Introduction

Investigations into microalgae focus on their function as sources of lipids for fuels and various goods, as their cultivation yields biomass rich in extractable cellular lipids. To assess a culture

for this objective, it is critical to take into account at least two distinct metrics: biomass concentration, which refers to the quantity of algal material per unit of culture volume, and lipid content, defined as the proportion of that biomass measured as lipid [1, 2]. A significant biomass density produces greater material for processing, whereas an elevated lipid ratio indicates a bigger lipid component in the collected material. No single statistic, when considered in isolation, reveals the fat content present in a litre of culture [3, 4, 5].

The differentiation is significant when the circumstances for culture promote growth and fat buildup in varying ways. A treatment that enhances biomass may reduce the observed lipid fraction, whereas a treatment that elevates lipid percentage can result in insufficient biomass to optimise lipid yield per culture volume. Research on microalgal culture has consequently assessed biomass generation in conjunction with lipid content and lipid-associated yield, rather than only considering the maximum lipid % as an adequate production benchmark [6, 7, 8, 9]. Rodolfi et al. [10] examined strain selection, lipid synthesis induction, and culture efficacy concurrently; similarly, Ho et al. [11] assessed biomass and lipid generation in Scenedesmus obliquus across several cultivation environments. Their research underscores the need for evaluating these elements, but the published figures are contingent upon the strain, culture method, test, and temporal framework employed [10, 11].

A further distinction pertains to concentration in contrast to production. Lipid concentration quantified in g L^{-1} denotes the quantity related to the volume of the sampled culture at a designated endpoint. Lipid yield, quantified in g L^{-1} d^{-1}, also considers the duration of culture. A lipid concentration derived from biomass and lipid percentage is pertinent for endpoint comparison; nevertheless, it does not directly measure harvested lipid, extraction efficiency,

triacylglycerol synthesis, or biodiesel yield [12, 13, 14]. A distinct differentiation of these criteria is essential when interpreting a cultural reaction into a suggested cultivation option. Nitrogen, phosphorus, and iron are significant for algal culture; yet, the documented reactions to their availability cannot be presumed to adhere to a singular pattern [15, 16, 17]. In experimental investigations concerning S. obliquus, the availability of nitrogen has influenced biomass production and lipid-associated results. Ho et al. [11] investigated nitrogen deprivation in conjunction with light intensity in an S. obliquus isolate and evaluated biomass, lipid, and carbohydrate yields. Breuer et al. [18] conducted a comparison of nitrogen-sufficient and nitrogen-deficient growth methods across nine microalgal strains, including S. obliquus, while assessing biomass and triacylglycerol accumulation. These results encourage the simultaneous investigation of growth and lipid responses. The current work does not demonstrate that a culture receiving a reduced nominal nitrogen dosage was nitrogen-deficient, as nutritional depletion and intracellular nitrogen levels were not assessed here [11, 18].

Phosphate studies indicate that the experimental environment is significant. Raj et al. [19] investigated the growth, metabolic reactions, and polyphosphate behaviour in freshwater microalgae, including S. obliquus, under varying phosphate availability. Guo et al. [20] examined the provision of phosphorus in S. obliquus UTEX 393 under conditions of nitrogen deprivation and observed impacts on growth, phosphorus allocation, and lipid synthesis. The combined nutritional circumstances cannot be regarded as equal to an independent phosphate dosage series performed under consistent background conditions [19, 20]. The availability of iron has also been examined as a factor in agriculture. Zhao et al. [21] assessed the impact of iron supplementation on biomass generation and lipid buildup in Scenedesmus sp. LX1 was cultivated in synthetic wastewater and residential secondary effluent. The medium and organism

utilised differ from those in the current experiment; nonetheless, the research demonstrates the necessity of evaluating iron dosage by both growth and lipid metrics. None of these studies provide clear proof of the physiological mechanisms functioning in the cultures examined; the existing dataset includes only endpoint biomass and lipid assessments, without data on nutrient absorption, intracellular nutrient reserves, or metabolic pathways.

A persistent issue in interpretation arises when research presents both the dosage that optimises biomass and the dosage that enhances lipid percentage, without assessing their combined effect. For instance, a culture exhibiting the highest lipid fraction may not always own the largest lipid quantity per litre if its biomass concentration is diminished [22, 23]. On the other hand, increased biomass from a larger fertiliser application may partially offset a decrease in lipid content. The pertinent comparison for the projected lipid quantity per culture volume is thus the biomass concentration multiplied by the lipid percentage, derived from measurements associated with each independently produced culture [24]. This computed endpoint must be understood within its constraints. The product of a culture's biomass concentration (g L^{-1}) and its lipid content as a fraction yields a computed lipid concentration (g L^{-1}). It fails to determine the quantity of lipid that would be retrieved post-harvesting and extraction, if the extract contains lipids appropriate for a certain product, or the rate at which the lipid was accumulated [25, 26].

Nonetheless, examining the three parameters of biomass concentration, lipid percentage, and anticipated lipid concentration may reveal if the proposed "optimal dosage" varies based on the objectives. Moreover, it permits the uncertainty inherent in the composite endpoint to undergo statistical examination when each separate culture is evaluated prior to averaging. Consequently, our research offers an evaluation centred on endpoints regarding the documented dosage

responses, rather than claiming the discovery of a new biochemical mechanism or a broadly applicable dietary guideline. The significance of pairwise evaluations of projected cholesterol levels is paramount: a higher average does not necessarily indicate that a dose is much more effective than its counterparts.

This investigation analysed the endpoint responses of Scenedesmus obliquus in three individual nutrient concentration series: nitrogen at 5, 10, 15, and 20 mg L^{-1}, phosphate at 1, 2, 3, and 4 mg L^{-1}, and iron at 0.5, 1.0, 1.5, and 2.0 mg L^{-1}. Each administration included three autonomously grown cultures, established with the same strain using analogous protocols and cultivation conditions. The concentration of biomass (g L^{-1}) and the lipid content (% of dry biomass were documented for each culture. The lipid concentration (g L^{-1}) was subsequently derived from the two associated measurements for every culture.

The objectives were to ascertain the variability of each assessed endpoint across doses within its nutrient series, evaluate if the amalgamation of biomass and lipid fractions altered the optimal dose for endpoint lipid content, and discern which dose variations were corroborated by statistical analyses within the series. Dose-mean biomass-lipid regressions were employed to elucidate relationships, avoiding the assignment of causation. The study does not evaluate the interactions between the nutrients, nor does it provide a unified nitrogen-phosphate-iron solution, as they were applied in separate orders.

2. Materials and methods

2.1. Strain identity, source and maintenance

The microalgal strain utilised in this study, *Scenedesmus obliquus* OSC, was previously isolated from fish ponds in southwestern Nigeria and documented in our earlier research [27]. Morphological characteristics and molecular analysis utilising 18S rRNA gene amplification and sequencing were employed to identify the strains. Each of the round, tapered cells of *Scenedesmus obliquus* OSC possessed a disc-like nucleus and a peripheral chloroplast. A molecular identification via 18S rRNA gene sequencing revealed a 99% identity with the *Scenedesmus obliquus* strain LU33 in the NCBI GenBank database [27]. Prior to use, the strain was maintained on Bold Basal Medium (BBM) agar plates at a temperature of 25 ± 2°C, pH 6.8, and subjected to a photoperiod of 16 hours of light and 8 hours of darkness. The identical S. obliquus culture was utilised consistently across the nitrogen, phosphate, and iron series. Three duplicates at each dosage were independently cultured cultures, established using analogous methodologies and identical growth circumstances, as verified for this work. Each culture served as the autonomous experimental unit, rather than a fraction or replicated instrument measurement. Articulating that unit expressly safeguards the interpretation of dosage comparisons against pseudoreplication [28].

2.2. Separate nitrogen, phosphate and iron dose-series design

Three distinct series of single-nutrient doses were performed with the identical S. obliquus culture and comparable growing methods. Nitrogen concentrations were evaluated at 5, 10, 15, and 20 mg L^{-1}; phosphate levels at 1, 2, 3, and 4 mg L^{-1}; and iron amounts at 0.5, 1.0, 1.5, and

2.0 mg L^{-1}. The dosage labels documented in the spreadsheet are as follows. Each dosage was administered to three separately developed cultures, resulting in 12 cultures per series and a total of 36 cultures. All three replicates followed identical protocols under the same documented growth circumstances and utilised the same strain. Biomass concentration and lipid content were individually documented for each culture at the conclusion. The dataset comprises a single pair of those values for every culture; the computed lipid concentration was then derived from each pair prior to dose-level summarisation and statistical evaluation. Dose evaluations were organised and analysed within each nutritional category. The configuration does not represent a factorial experiment including nitrogen, phosphate, and iron: it is incapable of assessing interactions between the nutrients or determining a collectively ideal medium.

2.3. Biomass concentration measurement and calculation

A precision balance (Precisa XB 220A) was employed to ascertain the desiccated mass of algae. The 10 mL microalgae culture suspension underwent centrifugation at 6000 xg for a duration of 15 minutes. Prior to measuring the dry weight, the collected algae are subjected to filtration using filter paper and subsequently washed with distilled water. Subsequently, the oven was employed for drying at 100 degrees Celsius for duration of 12 hours. Three replicas of each measurement were conducted. Upon completion of the culture processes, the entire microalgae biomass was centrifuged with a TD3 (800B) centrifuge for five minutes at 400 rpm. The algal biomass underwent three rounds of purification with distilled water, was thereafter dried in an oven, and then preserved at -20°C for further analysis to ensure complete extraction from the

nutritional medium [29]. The biomass concentration was determined gravimetrically, concentration was calculated as described below in equation (1):

$$X = [m_{dry} - m_{blank}] / V_{sample} \quad (1)$$

where X is biomass concentration (g L^{-1}), m_{dry} is the dry mass associated with the sampled biomass, m_{blank} is the mass of the empty collection vessel or filter, and V_{sample} is the sampled culture volume in litres. The description of each mass term should be adjusted to match the actual weighing procedure. One biomass value was retained for each independent culture for the dose-level summaries and analyses.

2.4. Lipid extraction, measurement and expression as percentage of dry biomass

Lipid extraction was conducted using the methodology outlined by Nascimento et al. [30]. A 2:1 proportion of synthesised methanol (2 mL) to chloroform (1 mL) was applied to 1 g of microalgal strains. To guarantee the complete dissolution of the lipids, the mixture was maintained at ambient temperature for a whole day. Subsequently, centrifugation was performed using the Benchtop EBA 200 Centrifuge for duration of ten minutes at a speed of 3000 rpm. The procedure was duplicated, and subsequent to the addition of two milliliters of chloroform, the pellet was vigorously agitated. The supernatant was isolated after an additional five-minute centrifugation at 300 rpm. Two distinct layers formed with the addition of 2 mL of 1% potassium chloride. The inferior segment with lipids and chloroform was collected independently in a test tube, whilst the superior segment with methanol and cells was poured out. A greater quantity of lipids was obtained by reiterating this procedure with the addition of 1 mL of potassium chloride, specifically targeting the top layer (methanol/cells). The first bottom layer (chloroform/lipid) was

combined with the subsequent bottom layer obtained from a repeated process to extract more lipids and then subjected to evaporation in a drying oven maintained at 80°C for 24 hours. The lipid content of a microalgal biomass was quantified as a percentage of its dry cell weight .For gravimetrically measured extract; lipid content was expressed using equation 2 shown below:

$$L = m_{lipid}/m_{biomass} \times 100 \quad (2)$$

where L is lipid content (% of dry biomass), m_{lipid}/ is the measured mass of recovered extract and $m_{biomass}$ is the dry biomass mass used for extraction.

2.5. Replicate-wise calculation of lipid concentration

An endpoint lipid concentration was calculated separately for each of the 36 independently cultivated cultures, using its paired biomass concentration and lipid-content measurements using equation (3) described below:

$$C_{lipid,i} = X_i (L_i/100) \quad (3)$$

where $C_{lipid,\,i}$ is calculated lipid concentration (g L^{-1}), X_i is biomass concentration (g L^{-1}) and L_i is lipid content (%) for culture i. The computation was executed prior to determining the mean and sample standard deviation for the three cultures at every dosage. Consequently, the calculated values maintain the association of the two measures within a culture; the multiplication of individual dose-level means was not employed as a replacement for replicate-level values. Computed lipid concentration quantifies the lipid quantity indicated by the assessed biomass and lipid fraction per litre of culture at the sampling conclusion. It differs from the directly assessed recovered lipid per litre, since it does not individually account for harvesting or

process-scale extraction losses. It is also differentiated from lipid productivity (g L^{-1} d^{-1}), which has a defined time frame. The concentrations determined at the three culture levels per dosage provided the results examined and compiled in Table 6.

2.6. Statistical analysis

The independently developed culture acted as the experimental unit (n=3 per treatment). The biomass concentration, lipid content, and assessed lipid concentration were compiled for each dosage as the arithmetic mean ± sample standard deviation (SD). The lipid concentration was initially acquired from the matched values of biomass and lipid content for each culture, as specified in Section 2.5. Each nutritional sequence was evaluated independently. For all three endpoints, a one-way analysis of variance (ANOVA) was employed to examine the effects of the four dosage levels, producing a total of nine ANOVAs. Every trial had 3 degrees of freedom between doses with 8 residual degrees of freedom. In cases of mean comparison, Tukey's honestly significant difference (HSD) approach offered multiplicity-adjusted pairwise comparisons for the nutrient–endpoint combination, applying $\alpha=0.05$. Means sharing a Tukey letter were not statistically separated at that threshold. Effect size was reported as **eta-squared**, $\eta^2=SS_{dose}$ /SS_{total}. In each nutrient series, ordinary least-squares regression delineated lipid content based on biomass concentration (g L^{-1}). Each regression utilised the four paired dosage-level averages (n=4; two residual degrees of freedom), rather than seeing the three cultures aggregated at each dose as twelve separate observations in the fitted model. The inclines were quantified as lipid-content percentage points per g L^{-1} of biomass, with R^2, slope-test p-values, and 95% confidence intervals presented in Table 5. Individual culture points were maintained in

Figure 3 to showcase variance within doses. The regressions depict correlations between dosages and were not utilised to infer a causal relationship of biomass on lipid levels.

3. Results and Discussion

3.1. Data structure and response measures

The information includes three types of nutrient applications for Scenedesmus obliquus: nitrogen, phosphate, and iron. Every series has four dosage phases, with three uniquely developed cultures associated with each phase. The cultures evolved under a stable environment characterised by constraints, pressures, and favourable developmental conditions. The autonomous culture necessitates three experimental iterations for every dosage; repeated observations or computations derived from a singular culture are not considered additional duplicates. The examined response variables included biomass concentration (g L^{-1}) and lipid content (% of dry biomass. Tables 1–3 present the mean values and standard deviations for each dosage level, whereas Figures 1 and 2 illustrate the significant reactions.

The lipid concentration alone does not accurately represent the quantity of lipid present in a certain culture volume. A culture may have an increased lipid concentration and a decreased biomass density. Consequently, a third endpoint lipid concentration (g L^{-1}) was systematically computed for each culture by using the formula of biomass concentration multiplied by lipid content divided by 100. The results at the cultural level for each dosage were then encapsulated as a mean and standard deviation in Table 6 and illustrated visually in Figure 4. Evaluating this endpoint before averaging preserves the correlation between biomass and lipid data obtained from the analogous culture. It furthermore permits the statistical analysis to employ three distinct

values for every dosage. This endpoint signifies an approximate lipid concentration per culture volume at the evaluated endpoint; it excludes lipid production, which requires a cultivation-time denominator. The variations in biomass synthesis, cellular lipid composition, and volumetric lipid output are crucial for understanding microalgal culture research [31, 32, 33].

The assessment of nitrogen, phosphate, and iron was carried out in four individual four-level dosage series. As a result, the comparisons underscore variations in dosages across a food sequence. The design is inadequate for conducting a factorial assessment of the interactions between nitrogen, phosphate, and iron, and it does not imply that nitrogen application is directly analogous to that of phosphate or iron. Accordingly, Table 4 presents distinct one-way analyses of variance for every response and nutrient series. Subsequent to the acknowledgment of a broad dose impact, the letter arrangements in Tables 1–3 and 6 convey Tukey-adjusted pairwise comparisons within that continuum. The related letters imply that the existing data failed to show a distinction at the specified significance level; they do not substantiate that the core replies are equivalent.

The three answers correspond to individual questions. Biomass concentration pertains to the overall mass of the culture, lipid content reflects the lipid segment of that mass, and determined lipid concentration integrates both in the final phase. It is important to analyse them together when their dosage plans are incompatible. These outcomes must likewise be analysed within the parameters of the lipid assay executed: the lipid levels obtained do not independently establish triacylglycerol concentrations, fatty acid profiles, or fitness for a particular metabolic function. The next subsections evaluate each nutritional group based on those parameters

Table 1: Biomass concentration and lipid content of *Scenedesmus obliquus* across the nitrogen dose series

Nitrogen concentration (mg L^{-1})	Biomass concentration (g L^{-1})	Lipid content (% dry biomass)
5	2.150 ± 0.030^{a}	77.03 ± 1.17^{a}
10	2.377 ± 0.025^{b}	69.30 ± 0.84^{b}
15	2.577 ± 0.025^{c}	61.25 ± 0.93^{c}
20	2.877 ± 0.025^{d}	51.58 ± 0.73^{d}

Table note: Values are mean ± sample SD from three independently cultivated cultures per nitrogen concentration n=3. Different superscript letters **within the same response column** indicate significant differences between concentrations by Tukey's honestly significant difference test ((p<0.05), following a separate one-way ANOVA for each response. Letters do not compare biomass with lipid content. **Statistical results:** Biomass, F(3,8)=407.67, p=4.38 $\alpha 10^{-9}$, η^2=0.994\); lipid content, F(3,8)=412.23, p=4.19 $\times 10^{-9}$, η^2=0.994. All six pairwise comparisons among nitrogen concentrations were significant for **each** response.

Table 2: Biomass concentration and lipid content of *Scenedesmus obliquus* across the phosphate dose series

Phosphate concentration (mg L^{-1})	Biomass concentration (g L^{-1})	Lipid content (% dry biomass)
1	2.063 ± 0.015^{a}	74.83 ± 0.70^{a}
2	2.300 ± 0.020^{b}	66.70 ± 0.46^{b}
3	2.523 ± 0.025^{c}	59.77 ± 0.35^{c}
4	2.777 ± 0.025^{d}	52.20 ± 0.36^{d}

Table note: Values are mean ± sample SD from three independently cultivated cultures per phosphate concentration n=3. Different superscript letters within the same response column indicate significant differences between concentrations by Tukey's honestly significant difference test (p<0.05), following a separate one-way ANOVA for each response. Letters do not compare biomass with lipid content.**Statistical results:** Biomass, F(3,8)=588.27,

$p=1.02 \times 10^{-9}$ $\eta^2=0.996$; lipid content, $F(3,8)=1171.78$, $p=6.54 \times 10^{-11}$, $\eta^2=0.998$. All six pairwise phosphate comparisons were significant for each response.

Table 3: Biomass concentration and lipid content of *Scenedesmus obliquus* across the iron dose series

Iron concentration (mg L^{-1})	Biomass concentration (g L^{-1})	Lipid content (% dry biomass)
0.5	2.110 ± 0.010^{a}	73.00 ± 0.20^{a}
1.0	2.363 ± 0.015^{b}	65.80 ± 0.30^{b}
1.5	2.600 ± 0.020^{c}	58.03 ± 0.15^{c}
2.0	2.863 ± 0.015^{d}	50.13 ± 0.25^{d}

Table note: Values are mean ± sample SD from three independently cultivated cultures per iron concentration (n=3). Different superscript letters within the same response column indicate significant differences between iron concentrations by Tukey's honestly significant difference test ($p<0.05$), following a separate one-way ANOVA for each response. Letters do not compare biomass with lipid content. **Statistical results:** Biomass, $F(3,8)=1290.15$, $p=4.45\times10^{-11}$, $\eta^2=0.998$; lipid content, $F(3,8)=5385.70$, $p=1.48\times10^{-13}$, $\eta^2=0.9995$. All six pairwise comparisons among iron concentrations were significant for each response.

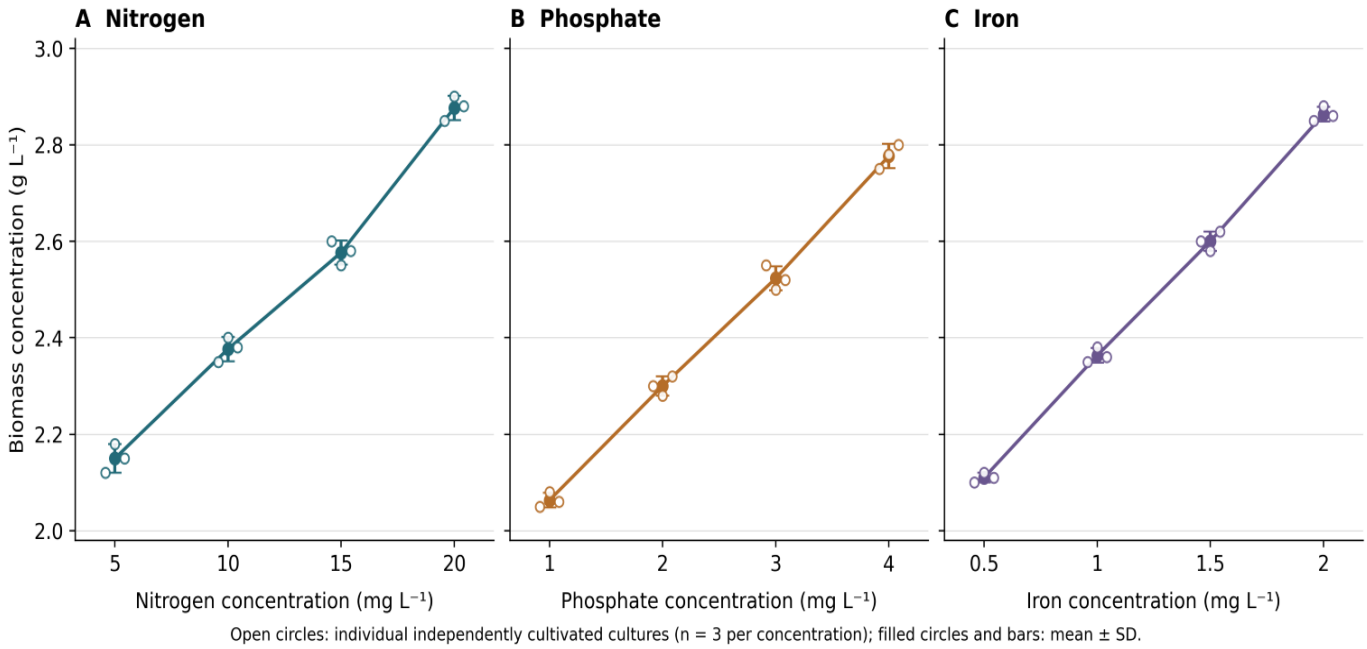


Figure 1: Biomass concentration of *Scenedesmus obliquus* across the (A) nitrogen, (B) phosphate and (C) iron dose series. Open circles show individual independently cultivated cultures (n=3) per concentration); filled circles and error bars show mean ± SD. Concentrations are labelled separately in each panel. Statistical comparisons within each series are reported in Tables 1–4.

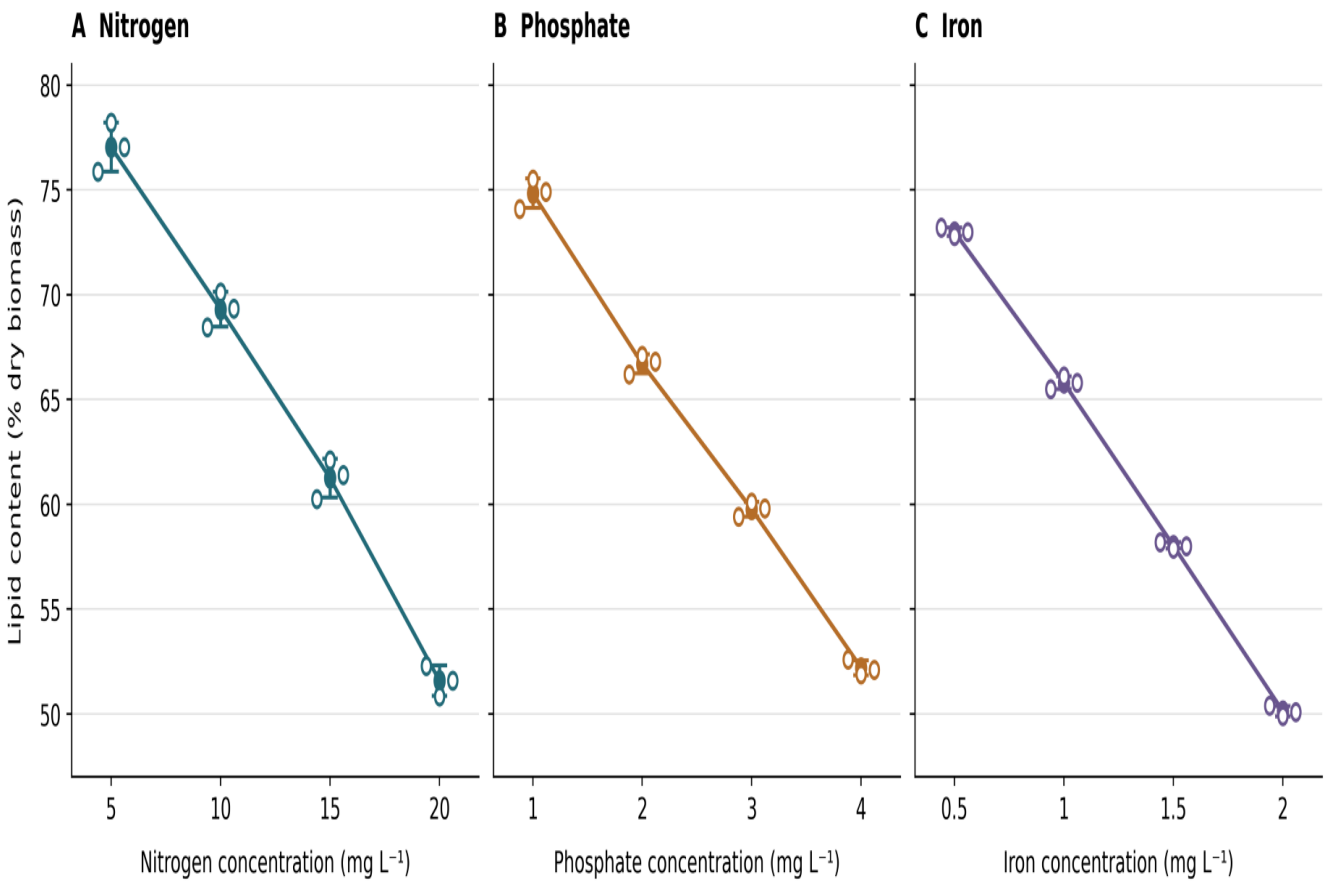


Figure 2: Lipid content of *Scenedesmus obliquus* across the (A) nitrogen, (B) phosphate and (C) iron dose series. Open circles represent individual independently cultivated cultures (n=3\) per concentration); filled circles and error bars represent mean ± SD. Each panel has its own concentration axis. Within-series statistical comparisons are reported in Tables 1–4.

3.2. Nitrogen dose response

The nitrogen dosage elicited contrasting patterns in the two observed reactions. Mean biomass concentration rose with each incremental dosage, starting from 2.150 ± 0.030 g L^{-1} at 5 mg L^{-1} to 2.877 ± 0.025 g L^{-1} at 20 mg L^{-1} (Table 1; Figure 1). This is an estimated increase of around

33.8% within the evaluated spectrum. The intermediate values, 2.377 ± 0.025 and 2.577 ± 0.025 g L^{-1} at 10 and 15 mg L^{-1}, respectively, indicate that the noted rise was spread throughout the dosage range instead of being limited to its extremes. Tukey comparisons designate several biomass categories for each of the four dosages (Table 1). The influence of nitrogen on biomass was notably significant in the independent one-way analysis, $F(3,8)=407.67$, $p=4.38 \times 10^{-9}$, and $\eta^2=0.9935$ (Table 4). Under the specified culture parameters and evaluated concentrations, 20 mg L^{-1} yielded the highest biomass density.

The lipid component migrated in the other way. The average lipid content decreased from 77.03 ± 1.17% at 5 mg L^{-1} to 51.58 ± 0.73% at 20 mg L^{-1}, representing a variation of 25.45 percentage points (Table 1; Figure 2). The averages at 10 and 15 mg L^{-1} were 69.30 ± 0.84% and 61.25 ± 0.93%, correspondingly. Each of the four dosages fell into separate Tukey groups for lipid content (Table 1), aligning with the comprehensive analysis, $F(3, 8)=412.23$, $p=4.19 \times 10^{-9}$ and $\eta^2=0.9936$ (Table 4). Consequently, the elevated biomass achieved with augmented nitrogen was correlated with a decreased lipid percentage recorded at each stage of this series.

This approach is physiologically credible, considering experimental findings that indicate nitrogen availability and deficiency might influence growth and fat buildup in S. obliquus. Ho et al. [11] investigated nitrogen deprivation in an S. obliquus isolate and assessed biomass, lipid, and carbohydrate yields, whereas Breuer et al. [18] analysed biomass and triacylglycerol responses in various microalgal strains, including S. obliquus, under both nitrogen-sufficient and deficient environments. The research endorses the consideration of nutrient availability as a factor influencing both growth and lipid-associated outcomes; however, the strains, culture methods, and lipid assessments vary from those utilised in the current study. The current dose-

response does not inherently indicate nitrogen famine, nitrogen depletion, a metabolic mechanism, or triacylglycerol accumulation: none of these were specifically assessed in this study [11, 18].

The pragmatic understanding shifts when biomass and fat components are included. The determined lipid concentrations were 1.656 ± 0.048, 1.647 ± 0.037, 1.578 ± 0.010, and 1.484 ± 0.008 g L^{-1} at 5, 10, 15, and 20 mg L^{-1}, respectively (Table 6; Figure 4). Despite the 5 mg L^{-1} treatment exhibiting the highest average, its determined lipid content was just around 0.009 g L^{-1} more than that at 10 mg L^{-1}. The reduction from 5 to 20 mg L^{-1} was around 10.4%, significantly less proportionate to the decrease in lipid percentage due to the compensatory effect of rising biomass on the diminishing lipid fraction. The influence of dosage on the computed lipid concentration was consistently observable, $F(3,8)=19.67$, $p=0.000475$, and $\eta^2=0.8806$ (Table 4).

The Tukey analysis categorises 5, 10, and 15 mg L^{-1} within the same letter group ("a"), whereas 20 mg L^{-1} is classified in group "b" (Table 6; Figure 4). Thus, the findings indicate a reduced estimated lipid concentration at 20 mg L^{-1} compared to each of the three lesser dosages, although they fail to pinpoint a statistically superior dose among 5, 10, and 15 mg L^{-1}. The numerical means remain distinct, and the comparison between 5 and 15 mg L^{-1} approaches the traditional threshold (p about 0.060); a common letter should not be construed as proof of equivalence. The justifiable conclusion is restricted to the examined range and endpoint, given that there are merely three independent cultures per dosage. The optimal nitrogen dosage yielded the highest biomass concentration. The lowest administered dosage had the most favourable results for lipid percentages. The computed endpoint lipid concentration revealed that the observed peak was at 5 mg L^{-1}; however, the three lower dosages were indistinguishable according to the Tukey test. An

assertion that 5 mg L^{-1} represents a singular production optimum, or that any intervention enhances lipid productivity to its fullest, needs additional substantiation.

3.3. Phosphate dose response

The lipid content exhibited a contrasting trend. It decreased from 74.83 ± 0.70% at 1 mg L^{-1} to 66.70 ± 0.46%, 59.77 ± 0.35%, and 52.20 ± 0.36% at the subsequent concentrations (Table 2; Figure 2). The disparity between the minimum and maximum dosages was 22.63 percentage points. Every phosphate dosage was categorised into an individual Tukey group for lipid content, and the cumulative impact was F(3,8)=1171.78, p=6.54×10-11, with η2=0.9977 (Table 4). The observed outcome indicates a progressive rise in culture biomass coupled with a corresponding decline in the fraction of that biomass identified as lipid. The substantial effect sizes indicate differentiation among the four administered dosages in these cultures; nevertheless, they do not determine the response pattern beyond this spectrum.

The lipid content exhibited a contrasting trend. It decreased from 74.83 ± 0.70% at 1 mg L^{-1} to 66.70 ± 0.46%, 59.77 ± 0.35%, and 52.20 ± 0.36% at the subsequent concentrations (Table 2; Figure 2). The disparity between the minimum and maximum dosages was 22.63 percentage points. Every phosphate dosage was categorised into an individual Tukey group for lipid content, and the cumulative impact was F(3,8)=1171.78, p=6.54×10-11, with η2=0.9977 (Table 4). The observed outcome indicates a progressive rise in culture biomass coupled with a corresponding decline in the fraction of that biomass identified as lipid. The substantial effect sizes indicate differentiation among the four administered dosages in these cultures; nevertheless, they do not determine the response pattern beyond this spectrum.

Combining the two measurements leads to a reduced dose response. The determined endpoint lipid concentrations were 1.544 ± 0.026, 1.534 ± 0.014, 1.508 ± 0.006, and 1.449 ± 0.008 g L^{-1} at 1, 2, 3, and 4 mg L^{-1}, respectively (Table 6; Figure 4). The recorded average decreased by around 6.1% from the minimum to the maximum dosage. The rise in biomass offsets a significant portion, but not the entirety, of the decrease in lipid content. The cumulative impact was statistically significant, $F(3,8)=22.44$, $p=0.000300$, $\eta 2=0.8938$ (refer to Table 4). The pairwise outcome is more detailed than the comprehensive test: 1, 2, and 3 mg L^{-1} belong to Tukey group “a”, whereas 4 mg L^{-1} is categorised in group “b” (Table 6). The data distinguishes the maximum dosage from each of the three lesser dosages concerning computed lipid concentration, although it fails to identify a singular optimal dose within the range of 1–3 mg L^{-1}. Specifically, the numerically highest mean of 1 mg L^{-1} needs to be referred to as an observed maximum rather than a statistically validated optimum.

Empirical studies validate that phosphorus availability can influence development and lipid-associated reactions in Scenedesmus, although they also indicate that a uniform response should not be presupposed [34, 35]. Raj et al. [36] investigated S. obliquus in conditions of reduced phosphate supply and noted changes in growth, biochemical composition, and polyphosphate dynamics. Yang et al. [37] investigated phosphate deficiency in a Scenedesmus sp. and documented increased lipid buildup alongside transcriptome alterations under their specific therapy. These investigations offer insight into the elevated lipid percentage seen at reduced phosphate levels; however, they do not confirm that the current cultures experienced phosphorus deficiency or that same molecular alterations transpired.

A divergent S. obliquus experiment is particularly beneficial for delineating the boundaries of comparison. Guo et al. [26] manipulated phosphorus availability during nitrogen deprivation in strain UTEX 393 and discovered that phosphorus levels influenced growth, phosphorus allocation, and lipid synthesis; increased phosphate supply might augment lipid content in that experimental context. This does not negate the reduction in lipid % during the current phosphate series. The nitrogen background, strain, phosphate levels, and treatment protocol dictate the nature of the comparison being conducted. It would be deceptive to amalgamate those data into a broad assertion that increased phosphate consistently elevates or decreases lipid accumulation [26].

In the current dataset, the selection of cultivation is contingent upon the endpoint. A dosage of four mg L^{-1} optimised the observed biomass concentration; one mg L^{-1} optimised the observed lipid percentage. The peak measured lipid content was also noted at 1 mg L^{-1}, although the disparity from 2 and 3 mg L^{-1} was not statistically significant (Tables 2 and 6; Figures 1, 2 and 4). No data on phosphate absorption, intracellular phosphorus levels, polyphosphate presence, or time-resolved lipid assessments were accessible to determine the physiological reason or an optimal productivity level. The endorsed conclusion indicates a dose-dependent relationship between biomass and lipid trade-off within the examined range, revealing a reduced lipid content at 4 mg L^{-1} compared to the other three concentrations.

3.4. Iron dose response

The highest recorded iron dose resulted in the most substantial biomass concentration; however, the peak anticipated lipid content occurred at a low level. Biomass rose from 2.110 ± 0.010 g L^{-1}

at a concentration of 0.5 mg L^{-1} to 2.363 ± 0.015, 2.600 ± 0.020, and 2.863 ± 0.015 g L^{-1} at doses of 1.0, 1.5, and 2.0 mg L^{-1}, respectively (Table 3; Figure 1). This signifies an anticipated increase of around 35.7% throughout the range. The various iron dose groups were differentiated using the biomass Tukey comparison (Table 3); the extensive analysis produced $F(3,8)=1290.15$, $p=4.45\times10^{-11}$, and $\eta^2=0.9979$ (Table 4). The results therefore demonstrate a consistently rising endpoint biomass concentration with each increase in iron dose.

The lipid content decreased simultaneously: 73.00 ± 0.20%, 65.80 ± 0.30%, 58.03 ± 0.15%, and 50.13 ± 0.25% at 0.5, 1.0, 1.5, and 2.0 mg L^{-1}, respectively (Table 3; Figure 2). The decrease from the first to the final dose amounted to 22.87 percentage points. The lipid content means for all four groups were differentiated by Tukey's test; the detailed analysis produced $F(3,8)=5385.70$, p=1.48×10-13, and η2 =0.9995 (Table 4). The little within-dose fluctuation and notable distinction define these independent cultures under the observed conditions. They should not be interpreted as proof that iron operates autonomously through a distinct metabolic pathway.

The multiplication of biomass concentration and lipid fraction accounts for the intermediate peak. The determined lipid content was 1.540 ± 0.003 g L^{-1} at 0.5 mg L^{-1}, which marginally rose to 1.555 ± 0.017 g L^{-1} at 1.0 mg L^{-1}, before decreasing to 1.509 ± 0.013 and 1.435 ± 0.002 g L^{-1} at 1.5 and 2.0 mg L^{-1}, respectively (Table 6; Figure 4). Between 0.5 and 1.0 mg L^{-1}, the almost 12.0% rise in average biomass significantly compensated for the reduction in lipid content from 73.0% to 65.8%; the overall increase in estimated lipid concentration was just 0.015 g L^{-1}, equating to around 1.0%. At elevated iron levels, the persistent reduction in lipid fraction surpassed the increase in biomass, resulting in a lipid concentration that fell below the averages of the lower dosages.

The statistical analysis is crucial for understanding this peak. The iron dosage influenced the overall estimated lipid content, $F(3,8)=69.98$, $p=4.40\times10^{-6}$, $\eta=0.9633$ (Table 4). In Table 6, the concentrations of 0.5 and 1.0 mg L^{-1} belong to Tukey group "a"; 1.5 mg L^{-1} is categorised as group "b", while 2.0 mg L^{-1} falls under group "c". The mean of 1.0 mg L^{-1} is the highest recorded value; nevertheless, it did not show a significant difference from 0.5 mg L^{-1} in the adjusted analysis (p about 0.408). Both the lower dosages surpassed the 1.5 and 2.0 mg L^{-1} levels, while the latter two were also differentiated from each other. Consequently, it would exaggerate the data to classify 1.0 mg L^{-1} as an exclusively ideal iron dosage. The most accurate outcome is a statistically indeterminate upper pair, succeeded by lower computed lipid values of 1.5 and 2.0 mg L^{-1}.

Empirical research indicates that iron supplementation can alter both biomass and lipid results in Scenedesmus, with the effective dose varying according to the organism and growth medium [38, 39, 40]. Zhao et al. [41] examined the incorporation of iron in Scenedesmus sp. LX1 between artificial wastewater and residential secondary effluent, assessing biomass yield and lipid buildup. Their context diverges from contemporary societies; thus, their reaction cannot provide a mechanical rationale or a substitute ideal for this strain [41].

The current findings indicate reactions to the administered iron dosages, rather than the iron that is really absorbed or its accessible portion. Iron speciation, precipitation, intracellular iron levels, photosynthetic performance, and oxidative stress were not assessed. Therefore, the decrease in lipid percentage should not be exclusively attributed to the alleviation of iron deficiency, iron toxicity, or modified carbon distribution without further substantiation. For the endpoint biomass target, a concentration of 2.0 mg L^{-1} yielded the highest average (Table 3; Figure 1). For lipid

concentration, 0.5 mg L⁻¹ yielded the highest average (Table 3; Figure 2). The computed endpoint lipid content reached a numerical peak of 1.0 mg L⁻¹, whereas 0.5 mg L⁻¹ was statistically comparable (Table 6; Figure 4). Replication at more granular dosages surrounding these two thresholds would be necessary prior to determining a more precise optimum.

3.5. Statistical magnitude and limits of the dose responses

The nine one-way analyses illustrated in Table 4 assess three endpoints: biomass concentration, lipid content, and estimated lipid concentration within the nitrogen, phosphate, and iron series. All omnibus tests discerned a distinction among the four dosages within their series. The data for biomass concentration, F(3,8), were recorded as 407.67 for nitrogen, 588.27 for phosphate, and 1290.15 for iron. The lipid content measurements were 412.23, 1171.78, and 5385.70, whereas the estimated lipid concentrations were 19.67, 22.44, and 69.98. Each of the nine reported p-values fell within 0.001 (Table 4). These evaluations indicate that the four approaches were not identical for any of the nine nutrient–endpoint pairs. The Tukey comparisons illustrated in Tables 1–3 and 6 offer clearer evidence for the dosages that were isolated.

The extent of the F statistics signifies both the difference in dosage means and the variance present across independent cultures receiving the same dose. This dataset had an atypically low degree of variance within doses. Within the twelve dosage groups, biomass standard deviations spanned from around 0.010 to 0.030 g L⁻¹, while the lipid-content standard deviations varied from around 0.15 to 1.17 percentage points. Since each group consists of just three cultures, these standard deviations are valuable indicators of the observed cultures but are unreliable estimates of the variance likely to occur in future civilisations. The procedures should clarify that each value was derived from a distinct culture and that the specified analytical precision

corresponds to the genuine measurement and reporting methodology. Safeguarding the independent culture as the replica mitigates the risk of inflating the sample size by regarding measurements from one culture as individual experimental units, a point highlighted by Hurlbert [28].

The presented η2 values demonstrate the extent to which the observed variance within series is ascribed to dosage in each one-way model. The values ranged from 0.9935 to 0.9979 for biomass, 0.9936 to 0.9995 for lipid content, and 0.8806 to 0.9633 for estimated lipid concentration (Table 4). The initial two endpoints exhibit notably pronounced differentiation among the assessed dosage averages in comparison to the variability within their respective dose categories. The diminished, although still considerable, values for computed lipid concentration align with the partial discrepancy between rising biomass and declining lipid percentage. The latter endpoint is derived from the two observed reactions, so its ANOVA provides a unique decision endpoint rather than an independent biological measurement.

These substantial impact sizes need a constrained interpretation. They delineate the twelve cultures and four concentrations within each series; nevertheless, they do not demonstrate comparably significant effects in an alternative strain, medium, cultivation size, or concentration spectrum. With n=3 for each dosage, the analyses possess just eight residual degrees of freedom, making the estimates of within-dose variability and η2 susceptible to an extra culture or an anomalous observation. The stated p-values are contingent upon the assumptions of one-way ANOVA, which encompass independence and proper handling of residual variance. Table 4 by itself cannot illustrate that the residual distributions or group variances meet those criteria. The

findings convincingly indicate separation in the documented experiment; however, enhanced accuracy and repeatability necessitate more independent cultures.

The nine omnibus tests focus on associated endpoints and were treated individually; Table 4 fails to offer a consolidated multiplicity-adjusted p-value for the entirety of the nine analyses. The text ought to maintain accurate p-values, observed variations, and effect sizes rather than associating a negligible p-value with practical relevance. Tukey letters for assessed lipid concentration reveal that statistically varied biomass and lipid percentage reactions do not invariably result in a different lipid concentration across all doses. The statistical evidence and the extent of an operationally relevant enhancement respond to separate queries, as underscored in the American Statistical Association's directives for p-value interpretation [42].

In conclusion, the F statistics, η2 values, and nominal dosage increments do not serve as reliable metrics for ordering nitrogen, phosphate, and iron in terms of biological "potency. Every nutrient was modified within varying concentration spectrums and has its own baseline and chemical significance. A 1 mg L^{-1} alteration in phosphate is not synonymous with a 1 mg L^{-1} alteration in nitrogen or iron, and the three series fail to segregate their influences within a shared factorial framework. An elevated F statistic for iron signifies a greater differentiation in relation to the fluctuations within the assessed iron series; it does not establish that iron is fundamentally more impactful than the other nutrients. This ranking would need a predefined similar scale, adequate shared controls, and a design that assesses nutrients in conjunction. Table 4 provides compelling evidence of dosage responses within the series, evaluated independently for each endpoint and nutrient.

Table 4: One-way ANOVA of biomass concentration, lipid content and calculated lipid concentration within each nutrient dose series

Nutrient series	Response	$df_{between}$	df_{within}	F	p	η^2
Nitrogen	Biomass concentration	3	8	407.67	4.38×10^{-9}	0.9935
Nitrogen	Lipid content	3	8	412.23	4.19×10^{-9}	0.9936
Nitrogen	Calculated lipid concentration	3	8	19.67	4.75×10^{-4}	0.8806
Phosphate	Biomass concentration	3	8	588.27	1.02×10^{-9}	0.9955
Phosphate	Lipid content	3	8	1171.78	6.54×10^{-11}	0.9977
Phosphate	Calculated lipid concentration	3	8	22.44	3.00×10^{-4}	0.8938
Iron	Biomass concentration	3	8	1290.15	4.45×10^{-11}	0.9979
Iron	Lipid content	3	8	5385.70	1.48×10^{-13}	0.9995
Iron	Calculated lipid concentration	3	8	69.98	4.40×10^{-6}	0.9633

Table note: Each ANOVA compares four concentrations **within one nutrient series**, using three independently cultivated cultures per concentration (N=12 per test). Calculated lipid concentration was obtained for each culture as biomass concentration × lipid content/100. Effect size was calculated as $\eta^2=SS_{between}/SS_{total}$. Pairwise results and group letters appear in Tables 1–3 and 6.

All nine omnibus tests indicate differences among concentrations within their respective series. The very large η^2 values for biomass and lipid content reflect strong separation among these four tested doses together with small within-dose variation. They should **not** be used to rank nitrogen, phosphate and iron by biological influence: the series have different dose ranges and were analysed separately. The calculated lipid-concentration tests also show why Table 6 matters—the effect on lipid mass per litre is less pronounced than the opposing changes in biomass and lipid percentage.

3.6. Biomass–lipid associations within each nutrient series

Table 5 and Figure 3 present the connection between biomass concentration and lipid content across the four dosage means in each nutrient series. Each regression utilised biomass and lipid-content values from three different cultures at a particular dosage, summarised as paired dose means; hence, the fitted line includes four points rather than twelve independent observations at various dose levels. Figure 3 likewise illustrates the separate culture findings, segmented by dosage. The three cultures at a certain dosage converge around their mean value. Demonstrating those cultures illuminates the internal dosage distribution, while adjusting the line to four dose averages ensures the reliability of the reported regression related to the dose-level question. The twelve presented cultural dimensions must not be characterised as twelve individual components in the regression evaluation.

The derived slopes were −35.34 for nitrogen, −31.65 for phosphate, and −30.58 for iron (see Table 5). Biomass is articulated in grams per litre (g L^{-1}), whereas lipid content is denoted as a percentage of the dry biomass. Therefore, each slope is measured in lipid-content percentage points for each 1 g L^{-1} increment in biomass concentration. According to the nitrogen fit, there is an estimated 3.53-percentage-point decline in mean lipid content for each 0.10 g L^{-1} elevation in mean biomass concentration across the four nitrogen dosage means observed. It does not specify a percentage drop in lipid concentration, a temporal variation rate, or the effects of experimentally increasing biomass while keeping the nutritional dosage unchanged. Indicating the units is vital, as the three slopes may otherwise be interpreted as dimensionless metrics of nutritional impact; the interpretation of regression coefficients is based on the scales employed for the variable measurements [43].

All three dose-level models exhibited a pronounced negative correlation. The coefficients of determination were R^2=0.9983 for nitrogen, 0.9989 for phosphate, and 0.9993 for iron; the corresponding slope-test p-values were 0.000864, 0.000553, and 0.000332 (Table 5). The 95% slope confidence ranges were from roughly −39.82 to −30.87, −34.86 to −28.45, and −32.98 to −28.18 percentage points per g L^{-1}. Consequently, when the administered nutrient dosage escalated and the mean biomass per dose climbed, the mean lipid percentage per dose diminished throughout all three series. Figure 3 illustrates the visual representation: the four groups advance toward increased biomass and reduced lipid content across each nutrition series.

The exceptionally elevated R2 values necessitate a focused interpretation. Every fit comprises only four dosage means and two residual degrees of freedom. Four systematic methods can closely approximate a linear relationship, even when the interaction among them varies beyond the examined range or under a different cultivation regime. The intervals and p-values encapsulate the fitted lines within the regression framework; they do not confirm linearity beyond the four sampled dosage levels. The small differences in the three R^2 values do not mean that any one nutrient has a more reliable or physiologically strong trade-off. The self-sustained duplicates facilitate the assessment of dosage averages and illustrate their variability; however, averaging them does not convert the four-dose regression into a large-sample correlation.

The correlation should not be construed as proof that the increase in biomass led to a reduction in lipid content. The dosage of nutrients fluctuated across each series, while biomass and lipid content were both evaluated as responses from the resultant cultures. Their adverse correlation may therefore emerge due to both reacting to fluctuating agricultural circumstances. The current approach fails to distinguish the direct impact of biomass from the influences of nutrient

availability or other growth-related processes. It lacks any quantification of nutrient absorption, intracellular nutrient conditions, carbon flow, or lipid-class production necessary to ascertain a process. Similarly, the gradients cannot be equated as causative influences of nitrogen, phosphate, and iron: their regressions illustrate distinct dosage sequences rather than interventions that provide a regulated, uniform alteration in biomass.

Table 5 and Figure 3 are therefore highly effective as a succinct representation of the contrasting measured responses. The trade-off demonstrated in Tables 1–3 is consistently evident across the four dosage means within each series. The endpoint comparison in Table 6 is not substituted; a decreasing lipid percentage with rising biomass may result in a little alteration, or perhaps a localised increase, in the computed lipid concentration. The iron series exemplifies this differentiation, showcasing its peak recorded lipid content at 1.0 mg L^{-1}, notwithstanding the adverse biomass–lipid-percentage gradient. Operational findings must consequently incorporate the endpoint pertinent to the cultivation objective, together with its cultural-level ambiguity and comparative analyses.

Table 5: Association between biomass concentration and lipid content across nutrient doses in *Scenedesmus obliquus*

Nutrient series	Dose-level means used (η)	Slope (% lipid per g L^{-1} biomass)	95% CI for slope	Intercept (%)	R^2	Regression p
Nitrogen	4	−35.34	−39.82 to −30.87	152.98	0.9983	0.000864
Phosphate	4	−31.65	−34.86 to −28.45	139.84	0.9989	0.000553
Iron	4	−30.58	−32.98 to −28.18	137.70	0.9993	0.000332

Table note: Within each nutrient series, ordinary least-squares regression was fitted to the **four concentration-level means** using lipid content (%) as the response and biomass concentration (g L^{-1}) as the predictor. Each mean represents three independently cultivated cultures. Slope confidence intervals use the regression standard error and (t) distribution with **2 residual degrees of freedom**. These regressions describe the observed dose-level trajectories; they do not establish that a change in biomass causes a change in lipid content.

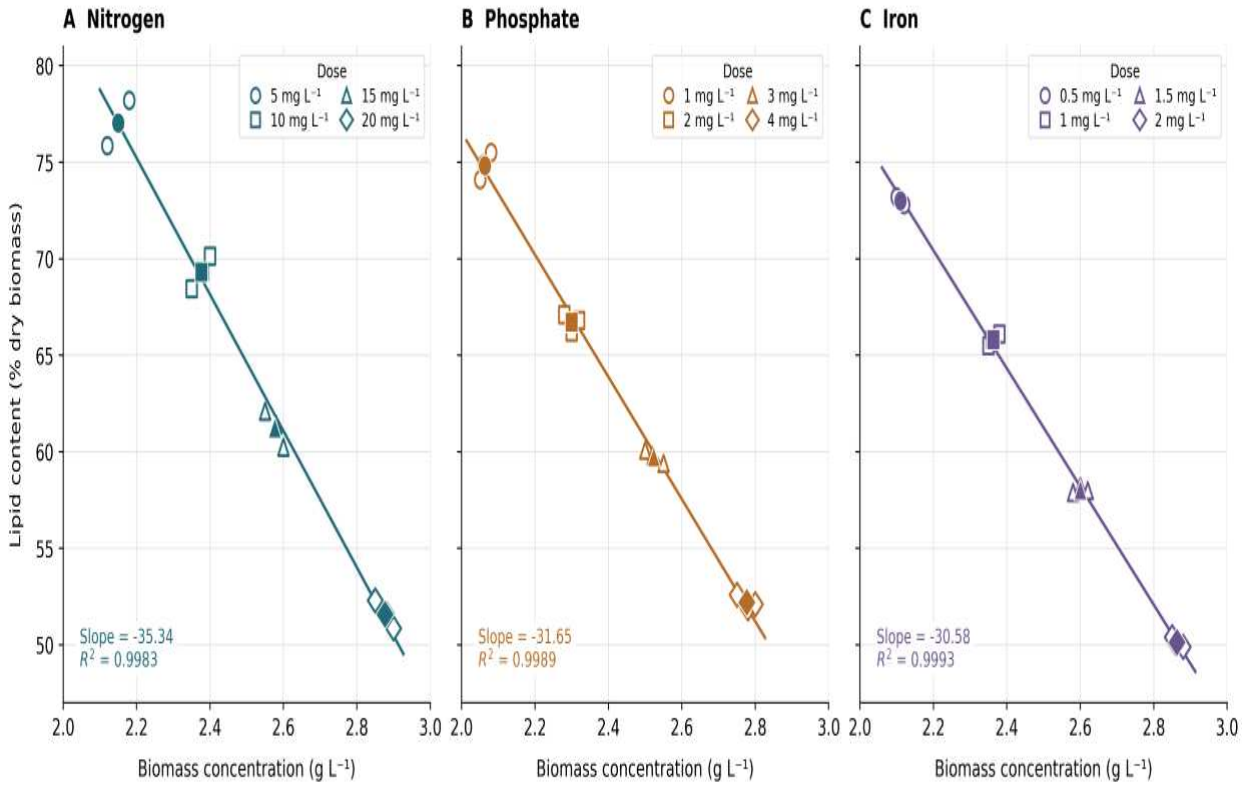


Figure 3: Association between biomass concentration and lipid content of *Scenedesmus obliquus* within the (A) nitrogen, (B) phosphate and (C) iron dose series. Marker shapes distinguish the four concentrations in each panel. Open markers represent individual independently cultivated cultures (n=3 per dose); filled markers represent dose-level means. Regression lines were fitted to the four means per nutrient series. Slopes and \R^2 correspond to Table 5 and describe associations, not a causal effect of biomass on lipid content.

3.7. Endpoint-dependent cultivation choice and study limitations

The optimal dosage is contingent upon the desired results of the cultivation procedure. For endpoint biomass concentration, the maximum evaluated dosage in each series yielded the highest average: 20 mg L^{-1} nitrogen (2.877 ± 0.025 g L^{-1}), 4 mg L^{-1} phosphate (2.777 ± 0.025 g L^{-1}), and 2.0 mg L^{-1} iron (2.863 ± 0.015 g L^{-1}; Tables 1–3). The minimal dosage examined in each series resulted in the highest average lipid content as a percentage of dry biomass: 5 mg L^{-1} nitrogen (77.03 ± 1.17%), 1 mg L^{-1} phosphate (74.83 ± 0.70%), and 0.5 mg L^{-1} iron (73.00 ± 0.20%; Tables 1–3). These represent many aims. Choosing a dosage based only on lipid % would neglect the biomass required to provide lipid per unit of culture volume.

The computed endpoint lipid concentration unifies the two observed responses. The peak recorded average was 5 mg L^{-1} nitrogen (1.656 ± 0.048 g L^{-1}), 1 mg L^{-1} phosphate (1.544 ± 0.026 g L^{-1}), and 1.0 mg L^{-1} iron (1.555 ± 0.017 g L^{-1}; Table 6; Figure 4). None of these numerical peaks determines a distinctly better dosage. In the nitrogen series, concentrations of 5, 10, and 15 mg L^{-1} belong to the same Tukey group for determined lipid levels; in the phosphate series, 1, 2, and 3 mg L^{-1} are grouped together. In the iron series, the recorded peak at 1.0 mg L^{-1} does not markedly differ from 0.5 mg L^{-1}. The maximum dosage evaluated in each series resulted in a markedly reduced estimated lipid concentration compared to the lower-dose group or groups indicated in Table 6. Consequently, the results identify specific dosages that should be reevaluated when the goal is to maximise volumetric lipid quantity, while also supporting ranges or statistically ambiguous pairings instead of three precise optimal lipid levels.

This classification is advantageous for decision-making processes. Should the immediate goal be biomass for a product that employs the complete algal material, the high-dose outcomes are

significant. If the aim is to obtain lipid-dense harvested biomass, the results regarding lipid content are relevant. Should the aim be to assess the lipid content in a litre of culture at the sampling endpoint, Table 6 is the relevant comparison. The three goals need to be delineated before utilising the term "ideal." The financial significance could fluctuate: a larger biomass might boost the requirements for harvesting and drying, while an augmented lipid percentage does not have to result in a higher lipid extraction from a stable culture volume. The outcomes of those processes were not assessed in this instance.

The assessed lipid concentration is a valuation, not an actual measurement of the bulk of the recovered product. Each culture's biomass concentration was multiplied by its corresponding lipid fraction to produce the result. The analysis is based on the premise that the biomass and lipid-content evaluations appropriately denote the same culture at the same terminal point. It does not individually address harvesting losses, extraction efficiency during processing, or later conversion losses. It ought not to be referred to as restored lipid yield. Lipid productivity cannot be determined in g L^{-1} d^{-1} without an established cultivation timeframe and time-specific production metrics. Investigations focusing on lipid yield or triacylglycerol generation concern interconnected but different outcomes and may not be considered direct corroboration of these assessed values [44, 45].

The current findings do not confirm biodiesel production. The total lipid content fails to indicate the specific lipid classes that were extracted, the proportion that might be transformed into fatty-acid methyl esters, or the quantity of biodiesel that could be generated from a culture. The dose-response data do not encompass transesterification yield, fatty-acid composition, or quantified fuel production. Assertions of enhanced biodiesel production or fuel excellence would

necessitate those evaluations. The computed lipid content of 1.656 g L^{-1} at 5 mg L^{-1} nitrogen should not be interpreted as a definitive g L^{-1} biodiesel yield by supposing complete extraction and conversion.

The experimental framework establishes an additional limitation. Nitrogen, phosphate, and iron were altered in distinct dosage series, each including four levels with three independently grown cultures per level. The outcomes allow for comparisons within each series based on its designated parameters. They fail to recognise interconnections between nutrients, an ideal nitrogen-phosphate-iron combination, or a justifiable hierarchy of nutrient effectiveness. Despite the numerical differences in the maximum computed lipid-concentration means across the three series, a direct comparison needs a shared, well-documented baseline and an experimental framework designed for that objective. The assessed ranges could also exclude a superior dosage that is beneath, within, or beyond the chosen thresholds. The minimal within-dose standard deviations indicate consistency among these cultures; nevertheless, further independent experimental trials are required to evaluate the stability of the rankings over time.

An intensive validation experiment should commence by assessing finer dosages surrounding the indeterminate top tiers, namely 5–15 mg L^{-1} nitrogen, 1–3 mg L^{-1} phosphate, and 0.5–1.0 mg L^{-1} iron, with supplementary separate cultures and a defined main endpoint. It must assess biomass and lipid proportions over time to enable the determination of lipid production and harvest scheduling. Simultaneous assessments of dissolved nutrient levels and, when relevant, intracellular nutritional conditions would elucidate if the specified doses indicate nutrient limitation or deficiency. The direct evaluation of extracted lipids per culture volume, in conjunction with lipid-class or fatty-acid characterisation and quantified methyl-ester synthesis,

would confirm if the final estimate predicts a viable product. Upon confirming the intra-series responses, a cohesive nutritional framework may evaluate interactions and formulate a strategy for the specified production objective.

Table 6: Calculated lipid concentration of *Scenedesmus obliquus* across separate nutrient dose series

Nutrient	Concentration (mg L^{-1})	Calculated lipid concentration (g L^{-1})
Nitrogen	5	1.656 ± 0.048^{a}
Nitrogen	10	1.647 ± 0.037^{a}
Nitrogen	15	1.578 ± 0.010^{a}
Nitrogen	20	1.484 ± 0.008^{b}
Phosphate	1	1.544 ± 0.026^{a}
Phosphate	2	1.534 ± 0.014^{a}
Phosphate	3	1.508 ± 0.006^{a}
Phosphate	4	1.449 ± 0.008^{b}
Iron	0.5	1.540 ± 0.003^{a}
Iron	1.0	1.555 ± 0.017^{a}
Iron	1.5	1.509 ± 0.013^{b}
Iron	2.0	1.435 ± 0.002^{c}

Table note: Values are mean ± sample SD of three independently cultivated cultures per concentration. Lipid concentration was calculated **separately for each culture** as biomass concentration (g L^{-1}) × lipid content (%)/100, then summarised. It is a calculated biomass-associated lipid concentration, not a separately measured lipid recovery. Within each nutrient series, means sharing a superscript letter do not differ significantly by Tukey's honestly significant difference test at ($p<0.05$). Letters are **not** comparisons between different nutrients.

Separate one-way ANOVA	(F(3,8))	(p)	(η^2)
Nitrogen	19.67	0.000475	0.881
Phosphate	22.44	0.000300	0.894
Iron	69.98	0.00000440	0.963

The largest observed nitrogen and phosphate means occur at their lowest tested concentrations, but their **first three concentrations share the same Tukey letter**. For iron, 1.0 mg L^{-1} has the largest observed mean; it does **not** differ significantly from 0.5 mg L^{-1} ((p=0.408)). The iron 1.5 and 2.0 mg L^{-1} groups differ from each other and from both lower-dose groups. Calculated lipid concentration was analysed separately within each nutrient series by one-way ANOVA, followed by Tukey's honestly significant difference test for pairwise comparisons (α=0.05).

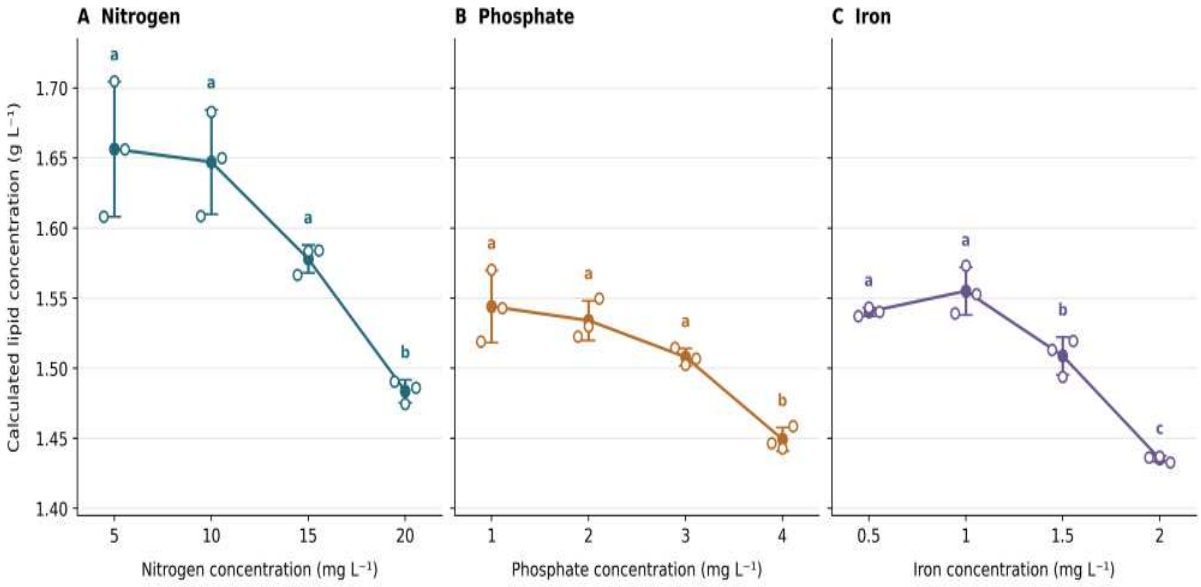


Figure 4: Calculated lipid concentration of *Scenedesmus obliquus* across the (A) nitrogen, (B) phosphate and (C) iron dose series. Lipid concentration was calculated for each independently cultivated culture as biomass concentration × lipid content/100. Open circles show individual cultures (\(n=3\) per dose); filled circles and error

bars show mean ± SD. Within each panel, concentrations sharing a letter do not differ significantly by Tukey HSD ((p<0.05)). Letters do not compare different nutrients. Full values are reported in Table 6.

4. Conclusion

This investigation filled a need in the assessment of nutrient-dose studies in Scenedesmus obliquus: the dose that generates the largest biomass or the highest lipid percentage does not have to yield the largest lipid volume per litre of culture. Throughout three individual four-dose series, rising concentrations of nitrogen, phosphate, or iron uniformly augmented endpoint biomass concentration while reducing lipid content. The peak assessed dosages resulted in 2.877 ± 0.025 g L^{-1} biomass with 20 mg L^{-1} nitrogen, 2.777 ± 0.025 g L^{-1} with 4 mg L^{-1} phosphate, and 2.863 ± 0.015 g L^{-1} with 2.0 mg L^{-1} iron. Conversely, the lowest administered dosages resulted in the greatest lipid percentages: 77.03 ± 1.17%, 74.83 ± 0.70%, and 73.00 ± 0.20%, respectively (Tables 1–3; Figures 1 and 2).

The main contribution consisted of calculating lipid concentration based on paired biomass and lipid measurements for each separate culture, thereafter doing a statistical comparison of that endpoint. The peak calculated concentrations were 1.656 ± 0.048 g L^{-1} for 5 mg L^{-1} nitrogen, 1.544 ± 0.026 g L^{-1} for 1 mg L^{-1} phosphate, and 1.555 ± 0.017 g L^{-1} for 1.0 mg L^{-1} iron (Table 6; Figure 4). These metrics reveal that the biomass-optimising dosages failed to optimise the anticipated lipid content per unit of culture volume. The results indicate a critical limitation in dose selection: Tukey comparisons did not differentiate nitrogen doses of 5, 10, and 15 mg L^{-1}, phosphate doses of 1, 2, and 3 mg L^{-1}, or iron doses of 0.5 and 1.0 mg L^{-1} for the lipid concentration determined. The identified maxima are thus not uniquely determined optimal values.

For scholars examining microalgal cultivation strategies, the outcomes endorse the collective reporting of biomass concentration, lipid percentage, and culture-level lipid concentration, along with pairwise uncertainty for the endpoint employed to direct a decision. This strategy averts the automatic classification of a significant lipid percentage or large biomass value as the superior volumetric lipid outcome. The result is limited by the experiment: each nutrient was analysed in a distinct series, including three cultures per dosage and one sampled endpoint. The interactions of nutrients, the stability of responses over culture iterations, and a blended medium formulation were not assessed. The determined lipid concentration does not evaluate recovered lipid, productivity adjusted by time, or biodiesel production.

Future investigations should evaluate smaller dosage variations within the statistically indeterminate groups through further independent cultures, analyse nutrient availability and biomass-lipid dynamics over time, and directly quantify the production of recovered lipids and methyl esters. An ensuing cooperative nutrient design may ascertain if the intra-series decisions provide a replicable formulation that boosts useable product yield.

CRediT authorship contribution statement

Abideen. A. Adekanmi: Conceptualisation, Design, Investigation, Methodology, Validation, visualization, writing the original draft , final Review & Editing

Emmanuel. O. Garuba: Conceptualisation, Investigation, Methodology, Review & Editing, Supvervision

Hidayat. A. Adekanmi: Conceptualisation, Resources, equipment's, Formal analysis Investigation, Methodology, final Review & Editing

Declaration of competing interest

The authors declare no conflicts of interest.

Clinical trial number: not applicable

Consent to Publish declaration: not applicable

Consent to Participate declaration: not applicable

Declaration of competing interest:

The authors declare no conflicts of interest.

Funding:

Financial assistance from public, private, or nonprofit funding organisations was not provided for this study. The authors state that this study was not supported by any particular grants.

Data Availability Statement:

This study's supporting data can be obtained from the corresponding author upon reasonable request.

Ethics approval statement:

Not applicable

Patient consent statement:

Not applicable

Clinical trial registration:

Not applicable

REFERENCES

[1] Fernandes T, Cordeiro N. Microalgae as Sustainable Biofactories to Produce High-Value Lipids: Biodiversity, Exploitation, and Biotechnological Applications. Mar Drugs. 2021 Oct 14;19(10):573. doi: 10.3390/md19100573. PMID: 34677472; PMCID: PMC8540142.

[2] Babu, S. S., Gondi, R., Vincent, G. S., JohnSamuel, G. C., & Jeyakumar, R. B. (2022). Microalgae Biomass and Lipids as Feedstock for Biofuels: Sustainable Biotechnology Strategies. *Sustainability*, *14*(22), 15070. https://doi.org/10.3390/su142215070

[3] Florea EC, Niculescu AG, Bratu AG, Mihaiescu DE, Grumezescu AM. Process Engineering Strategies for Microbial Lipid Production: From Strain Evolution to Industrial-Scale Bioprocessing. Int J Mol Sci. 2026 Apr 23;27(9):3760. doi: 10.3390/ijms27093760. PMID: 42123346; PMCID: PMC13164146.

[4] Ivanisevic, M., He, S., Duboriz, I. *et al.* Biomethane and biomethanol fermentation can produce microbial lipids at competitive selling prices. *Commun. Sustain.* **1**, 101 (2026). https://doi.org/10.1038/s44458-026-00104-z

[5] Polat, Z., Sayın, B., Kaya, M., & Kaban, G. (2026). Optimization of Biomass and Lipid Production by *Yarrowia lipolytica* Using Flaxseed and Chia Seed Oils as Substrates. *Fermentation*, *12*(3), 169. https://doi.org/10.3390/fermentation12030169

[6] Cabrera-Capetillo, C. A., Castillo-Baltazar, O. S., Peña-Caballero, V., Petriz-Prieto, M. A., Guzmán-López, A., Valdovinos-García, E. M., & Bravo-Sánchez, M. G. (2025). Evaluation of Biomass, Lipid and Chlorophyll Production of a Microalgal Consortium Cultured in Dairy Wastewater. *Fermentation*, *11*(9), 506. https://doi.org/10.3390/fermentation11090506

[7] Adekanmi, A.A., Garuba, E.O., Onilude, A.A. *et al.* Biomass optimisation and scale-up in photobioreactor by *Pediastrum duplex* strain KT 003362.1 to produce microalgal lipids for biodiesel production. *Discov Sustain* **7**, 993 (2026). https://doi.org/10.1007/s43621-026-03910-6

[8] Park SB, Lee YR, Yun JH, Choi HI, Sim EJ, Choi DY, Cho DH, Kim HS, Lee YJ. Towards maximizing biomass and lipid productivity: high-throughput screening assay for prospecting heterotrophic growth for new microalgal isolates. Microb Cell Fact. 2024 Nov 8;23(1):299. doi: 10.1186/s12934-024-02550-7. PMID: 39511591; PMCID: PMC11545793.

[9]

Udayan A, Pandey AK, Sirohi R, Sreekumar N, Sang BI, Sim SJ, Kim SH, Pandey A. Production of microalgae with high lipid content and their potential as sources of nutraceuticals. Phytochem Rev. 2022 Jan 23:1-28. doi: 10.1007/s11101-021-09784-y. Epub ahead of print. PMID: 35095355; PMCID: PMC8783767.

[10] Rodolfi L, Chini Zittelli G, Bassi N, Padovani G, Biondi N, Bonini G, Tredici MR. Microalgae for oil: strain selection, induction of lipid synthesis and outdoor mass cultivation in a low-cost photobioreactor. Biotechnol Bioeng. 2009 Jan 1;102(1):100-12. doi: 10.1002/bit.22033. PMID: 18683258.

[11] Ho SH, Chen CY, Chang JS. Effect of light intensity and nitrogen starvation on CO2 fixation and lipid/carbohydrate production of an indigenous microalga Scenedesmus obliquus CNW-N. Bioresour Technol. 2012 Jun;113:244-52. doi: 10.1016/j.biortech.2011.11.133. Epub 2011 Dec 8. PMID: 22209130.

[12] Raya MPP, Martínez Cartas ML, Sánchez S. Lipid Extraction and Cell Disruption Methods for Improving Biodiesel Production by *Scenedesmus sp*. Microorganisms. 2026 Mar

24;14(4):731. doi: 10.3390/microorganisms14040731. PMID: 42075128; PMCID: PMC13118601.

[13] Alsaadi, S., Ahmad, M.I. & Shakir, M.A. Kinetics and thermodynamics study of lipid extraction from *Camelus dromedarius* fat waste and feedstock application in biodiesel production. *Discov Sustain* **6**, 1102 (2025). https://doi.org/10.1007/s43621-025-01992-2

[14] Bradley, T., Rajaeifar, M.A., Kenny, A. *et al.* Life cycle assessment of microalgae-derived biodiesel. *Int J Life Cycle Assess* **28**, 590–609 (2023). https://doi.org/10.1007/s11367-023-02140-6

[15] Yaakob MA, Mohamed RMSR, Al-Gheethi A, Aswathnarayana Gokare R, Ambati RR. Influence of Nitrogen and Phosphorus on Microalgal Growth, Biomass, Lipid, and Fatty Acid Production: An Overview. Cells. 2021 Feb 14;10(2):393. doi: 10.3390/cells10020393. PMID: 33673015; PMCID: PMC7918059.

[16] Myrstener, M., Fork, M.L., Bergström, AK. *et al.* Resolving the Drivers of Algal Nutrient Limitation from Boreal to Arctic Lakes and Streams. *Ecosystems* **25**, 1682–1699 (2022). https://doi.org/10.1007/s10021-022-00759-4

[17] Seelen EA, Gleich SJ, Kumler W, Anderson HS, Bian X, Björkman KM, Caron DA, Dyhrman ST, Ferrón S, Finkel ZV, Haley ST, Hu YY, Ingalls AE, Irwin AJ, Karl DM, Kong KP, Lowenstein DP, Salazar Estrada AE, Townsend E, Tracey JC, Turk-Kubo K, Van Mooy BAS, John SG. Nitrogen and phosphorus differentially control marine biomass production and stoichiometry. Nat Commun. 2025 Jul 1;16(1):5713. doi: 10.1038/s41467-025-61061-0. PMID: 40595531; PMCID: PMC12219287.

[18] Breuer G, Lamers PP, Martens DE, Draaisma RB, Wijffels RH. The impact of nitrogen starvation on the dynamics of triacylglycerol accumulation in nine microalgae strains. Bioresour Technol. 2012 Nov;124:217-26. doi: 10.1016/j.biortech.2012.08.003. Epub 2012 Aug 10. PMID: 22995162.

[19] Raj S, Sreenikethanam A, Gobi M, Sakate D, Jayakumar T, Rakesh S, Banu JR, Bajhaiya AK. Effect of phosphate availability on the dynamics of polyphosphate accumulation in microalgae. Sci Rep. 2025 Nov 7;15(1):39069. doi: 10.1038/s41598-025-24985-7. PMID: 41203826; PMCID: PMC12594759.

[20] Guo L, Wu Q, Lai YS, Eustance E, Rittmann BE. Revealing the role of phosphorus supply on the phosphorus distribution and lipid production in Scenedesmus obliquus UTEX 393 during nitrogen starvation. Sci Total Environ. 2023 Feb 1;858(Pt 1):159811. doi: 10.1016/j.scitotenv.2022.159811. Epub 2022 Oct 28. PMID: 36349625.

[21] **Zhao, W. Y., Yu, J. Y., Wu, Y. H., Hong, Y., & Hu, H. Y. (2014). Enhancement of** *Scenedesmus* sp. LX1 biomass production and lipid accumulation using iron in artificial wastewater and domestic secondary effluent. ***Microbiology and Biotechnology Letters***, **42(2), 131–138. DOI:** 10.4014/kjmb.1312.12004

[22] Banskota AH, Stefanova R, Hui JPM, Bermarija T, Stemmler K, McGinn PJ, O'Leary SJB. Comprehensive Analysis of Biomass from *Chlorella sorokiniana* Cultivated with Industrial Flue Gas as the Carbon Source. Molecules. 2024 Jul 18;29(14):3368. doi: 10.3390/molecules29143368. PMID: 39064946; PMCID: PMC11279589.

[23] Montoya-Vallejo C, Guzmán Duque FL, Quintero Díaz JC. Biomass and lipid production by the native green microalgae *Chlorella sorokiniana* in response to nutrients, light intensity, and carbon dioxide: experimental and modeling approach. Front Bioeng Biotechnol. 2023 May 17;11:1149762. doi: 10.3389/fbioe.2023.1149762. PMID: 37265992; PMCID: PMC10229873.

[24] Fais G, Castelli S, Dessì D, Perra G, Lai N, Cao G, Concas A. *Chlorella vulgaris* lipid extraction side-stream enhances growth and protein enrichment in novel food *Lemna minor* (duckweed). Front Nutr. 2026 May 29;13:1822150. doi: 10.3389/fnut.2026.1822150. PMID: 42293216; PMCID: PMC13259828.

[25] Griffiths MJ, van Hille RP, Harrison ST. The effect of nitrogen limitation on lipid productivity and cell composition in Chlorella vulgaris. Appl Microbiol Biotechnol. 2014 Mar;98(5):2345-56. doi: 10.1007/s00253-013-5442-4. Epub 2014 Jan 12. PMID: 24413971.

[26] Gao B, Hong J, Chen J, Zhang H, Hu R, Zhang C. The growth, lipid accumulation and adaptation mechanism in response to variation of temperature and nitrogen supply in psychrotrophic filamentous microalga Xanthonema hormidioides (Xanthophyceae). Biotechnol Biofuels Bioprod. 2023 Jan 19;16(1):12. doi: 10.1186/s13068-022-02249-0. PMID: 36658609; PMCID: PMC9854199.

[27] Adekanmi, A.A., Onilude, A.A., Garuba, E.O., Adegboye, M.A. (2025). Screening, Morphological and Molecular Identification of Indigenous Microalgal Strains for Biodiesel Production, *International Journal of Engineering and Information system,* Vol. 9, Issue 1: 59-71.

[28] Hurlbert, S. H. (1984). Pseudoreplication and the design of ecological field experiments. *Ecological Monographs*, 54(2), 187-211

[29] Zhu, C.J. and Lee, Y.-K., 1997. Determination of biomass dry weight of marine microalgae. *Journal of Applied Phycology*, 9(2), pp.189–194.

[30] Nascimento, I. A., Marques, S. S. I., de Souza, I. T. D., Prudêncio, I. R., de Carvalho, A. B., & dos Santos, J. A. (2013). Screening of microalgae strains for biodiesel production: Lipid extraction efficiency and fatty acid profile optimization. *Energy & Fuels*, 27(12), 7437–7446.

[31] Yang L, Duan B and Lu Q (2025) A review of marine microalgae-based lipids production: biosynthesis, technological advancements, and practical applications. Front. Nutr. 12:1664674. doi: 10.3389/fnut.2025.1664674

[32] Adekanmi, A.A., Garuba, E.O., Muraina, T.A. *et al.* Design and experimental evaluation of an internally illuminated hybrid mixing photobioreactor for intensified microalgal biodiesel production with techno-economic and scale-up assessment. *Discov Biotechnol* **3**, 13 (2026). https://doi.org/10.1007/s44340-026-00060-3

[33] Je S, Yamaoka Y. Biotechnological Approaches for Biomass and Lipid Production Using Microalgae *Chlorella* and Its Future Perspectives. J Microbiol Biotechnol. 2022 Nov

28;32(11):1357-1372. doi: 10.4014/jmb.2209.09012. Epub 2022 Oct 21. PMID: 36310359; PMCID: PMC9720082.

[34] Qari, H. A., Al-Shaeri, M. A., & Oves, M. (2024). Effect of Phosphorus Deprivation on Fatty Acid Synthesis in *Scenedesmus subspicatus* Microalgae from Rostherne Mere. *Fuels*, *5*(4), 910-926. https://doi.org/10.3390/fuels5040051

[35] Parmar P, Kumar R, Neha Y and Srivatsan V (2023) Microalgae as next generation plant growth additives: Functions, applications, challenges and circular bioeconomy based solutions. Front. Plant Sci. 14:1073546. doi: 10.3389/fpls.2023.1073546

[35] Raj S, Sreenikethanam A, Gobi M, Sakate D, Jayakumar T, Rakesh S, Banu JR, Bajhaiya AK. Effect of phosphate availability on the dynamics of polyphosphate accumulation in microalgae. Sci Rep. 2025 Nov 7;15(1):39069. doi: 10.1038/s41598-025-24985-7. PMID: 41203826; PMCID: PMC12594759.

[37] Yang F, Xiang W, Li T, Long L. Transcriptome analysis for phosphorus starvation-induced lipid accumulation in Scenedesmus sp. Sci Rep. 2018 Nov 6;8(1):16420. doi: 10.1038/s41598-018-34650-x. PMID: 30401886; PMCID: PMC6219579.

[38] Tao, R., Bair, R., Lakaniemi, AM. *et al.* Use of factorial experimental design to study the effects of iron and sulfur on growth of *Scenedesmus acuminatus* with different nitrogen sources. *J Appl Phycol* **32**, 221–231 (2020). https://doi.org/10.1007/s10811-019-01915-5

[39] Lisa Aditya, Viet Q. Ly, Md Abu Hasan Johir, Unnikrishnan Kuzhiumparambil, Peter J. Ralph, Long D. Nghiem; Growth response of *Scenedesmus* and *Chlorella* to elevated sulfate concentrations. *Environ. Sci.: Water Res. Technol.* 2026; 12 (5): 1548–1558. https://doi.org/10.1039/d5ew01288k

[40] Abidizadegan M, Blomster J and Peltomaa E (2023) Effect of micronutrient iron on bioactive compounds isolated from cryptophytes. Front. Plant Sci. 14:1208724. doi: 10.3389/fpls.2023.1208724

[41] Zhao, W.-Y., Yu, J.-Y., Wu, Y.-H., Hong, Y., & Hu, H.-Y. (2014). Enhancement of *Scenedesmus* sp. LX1 Biomass Production and Lipid Accumulation Using Iron in Artificial Wastewater and Domestic Secondary Effluent. *Microbiology and Biotechnology Letters* ***42***(2), 131–138. [**DOI:** 10.4014/kjmb.1312.12004

[42] Wasserstein, R. L., & Lazar, N. A. (2016). The ASA's statement on p-values: Context, process, and purpose. *The American Statistician*, ***70***(2), 129–133. https://doi.org/10.1080/00031305.2016.1154108

[43] Schielzeth, H. (2010). Simple means to improve the interpretability of regression coefficients. *Methods in Ecology and Evolution*, ***1***(2), 103–113. doi.org

[44] Du F, Xu Q, Li X, Hang Y, Zhang D, Zhang F, Ma W, Sun X, Huang H. Regulating triacylglycerol cycling for high-efficiency production of polyunsaturated fatty acids and derivatives. Nat Commun. 2025 May 8;16(1):4262. doi: 10.1038/s41467-025-59599-0. Erratum in: Nat Commun. 2025 Nov 21;16(1):10314. doi: 10.1038/s41467-025-66665-0. PMID: 40335511; PMCID: PMC12059026.

[45]Ferrer-Ledo N, Stegemüller L, Janssen M, Wijffels RH and Barbosa MJ (2023) Growth and fatty acid distribution over lipid classes in Nannochloropsis oceanica acclimated to different temperatures. Front. Plant Sci. 14:1078998. doi: 10.3389/fpls.2023.1078998